Cancer Management and Research

Dovepress

open access to scientific and medical research

Open Access Full Text Article

ORIGINAL RESEARCH

Human Chorionic Gonadotropin Polypeptide Nanoparticle Drug Delivery System Improves Methotrexate Efficacy in Gestational Trophoblastic Neoplasia in vitro

This article was published in the following Dove Press journal:
Cancer Management and Research

Qing Cong[1,2,*]
Ling Lin[1,3,*]
Biao Qi[4]
Congjian Xu[1,2]
Xiaoyan Zhang[1,2]

[1]Obstetrics and Gynecology Hospital, Fudan University, Shanghai, People's Republic of China; [2]Shanghai Key Laboratory of Female Reproductive Endocrine Related Diseases, Shanghai, People's Republic of China; [3]Institutes of Biomedical Sciences of Shanghai Medical School, Fudan University, Shanghai, People's Republic of China; [4]Xiamen Branch, Zhongshan Hospital, Fudan University, Xiamen, People's Republic of China

*These authors contributed equally to this work

Purpose: To alleviate the sufferings of the chemotherapy patients, we developed a novel active targeted therapeutic system and showed its potential as a promising drug delivery strategy.

Methods: We utilized the human chorionic gonadotropin (HCG) ligand-receptor mediation to make an actively targeted drug delivery system with optimal HCG polypeptide fragment as target head base, polyethylene glycol–polylactic acid copolymers as nanometer materials to load chemotherapy drug methotrexate (MTX), to highly selectively deliver MTX into choriocarcinoma lesions, and to investigate the efficacy, targeting and tolerability of the complex in vitro experiments.

Results: Our data show that choriocarcinoma cell lines JEG-3 and JAR exhibited high expression levels of HCG receptor, peptide HCGβ81-95 specifically bonded to HCG receptor-positive cells and HCG81-NP efficiently delivered MTX to choriocarcinoma cells. HCG81-NP-MTX inhibited cell proliferation and reduced G_0/G_1 to S phase transition in JEG-3 and JAR cells.

Conclusion: We designed an active targeting therapy system of choriocarcinoma, significantly improved chemotherapy efficacy in vitro, and provided a theoretical basis for the treatment of malignant trophoblastic tumors.

Keywords: choriocarcinoma, human chorionic gonadotropin, nanoparticle, methotrexate, cell proliferation

Introduction

Methotrexate (MTX) is a first-line chemotherapy agent in treating gestational trophoblastic neoplasia (GTN) and ectopic pregnancy.[1–3] MTX is also one of the most widely used anticancer agents for the treatment of a broad range of tumors including lung, breast, ovarian, head and neck, leukemia, lymphoma, osteosarcoma, and bladder cancer.[4–7] Efficacy of MTX-mediated chemotherapy requires sufficient amount and specific targeting to tumor cells. Because of lack of drug distribution selection, traditional choriocarcinoma chemotherapy results in a dramatic systemic adverse reaction, drug resistance and even recurrence problems.[8]

Nanotechnology provides opportunities to design and develop nanoparticles for specific biomedical applications, such as target, diagnose, image and treat devastating diseases such as cancer.[9,10] Nanoparticle delivery systems can release the

Correspondence: Congjian Xu; Xiaoyan Zhang
Department of Gynecology, Obstetrics and Gynecology Hospital, Fudan University, Shanghai, 200011, People's Republic of China
Email xucj@hotmail.com; zhxy@fudan.edu.cn

submit your manuscript | www.dovepress.com
DovePress
http://doi.org/10.2147/CMAR.S279831

specific drug into the targeted sites based on the specific binding of certain modified small molecules to targeted cells.[11,12] The combination of the active targeting system and nanoparticle carriers can not only target specifically tumor foci but also deliver more drugs to those sites.[13]

In our previous study, an active polypeptide-nanoparticles-paclitaxel system displayed stronger anti-proliferation and anti-tumor effects. Our nanoparticles also exhibited higher selectivity and efficacy compared with free paclitaxel or naked paclitaxel-loaded nanoparticles both in vitro and in vivo. Poly (lactic acid) (PLA) nanoparticles with the surface modifications of poly (ethylene glycol) (PEG) and methoxy-PEG (MPEG) could enable PLA nanoparticles to escape uptake by the mononuclear phagocytic system so as to prolong its blood half-life.[14,15] In particular, nanoparticle delivery system showed a high degree of selectivity and treatment efficacy for ovarian cancer management.[13,16]

GTN is common gynecological disease that can not only produce large amounts of human chorionic gonadotropin (HCG) but highly expressed HCG receptor (official full name: luteinizing hormone/choriogonadotropin receptor, LHCGR).[17,18] In healthy women, LHCGR is mainly located in female reproductive organs including uterus, ovarian and fallopian tubes, but rarely expressed in other normal tissues.[19,20] LHCGR is thus proven to be an optimal target for GTN diagnosis and therapy. HCG-modified nanoparticles for choriocarcinoma therapy have seldom been reported. Compared with HCGβ1-15, LHβ41-55 and LHβ91-105, HCGβ81-95 polypeptide (HCG81) has better binding potency with LHCGR.[21] Hence, we investigated the potential of HCGβ81-95 polypeptide-conjugated PEG-PLA nanoparticles (HCG81-NP) as a novel drug delivery system to treat GTN.

Materials and Methods

Cell Lines and Experimental Mice

As research models, human oral keratinocytes (HOK) were purchased from ScienCell (California, USA). Primary human coronary artery smooth muscle cell (HCASMC) was purchased from PromoCell (Heidelberg, Germany). The human monocytic cell line THP-1 and human embryonic kidney 293 (HEK-293) cells were purchased from the cell bank of Chinese Academy of Sciences (Shanghai, China). The human trophoblast cell line HTR8/sev8 was purchased from JENNICO Biological Technology (Guangzhou, China). The human choriocarcinoma cell lines JEG-3 and JAR, human ovarian cancer cell line Caov-3 were also obtained from the cell bank of Chinese Academy of Sciences. All these were obtained within 6 months before being used in this study. These cell lines were cultured in DMEM or RPMI 1640 medium (Gbico) containing 10% fetal bovine serum (Gibco), 100 IU/mL penicillin G and 100 mg/mL streptomycin sulfate (Hyclone). As for HCASMC, primary cells were cultured in smooth muscle cell medium containing 2% fetal bovine serum and smooth muscle cell growth supplement (ScienCell).

All experimental animal procedures were approved by the Animal Care and Use Committee of Fudan University, which followed the guidelines for the ethical review of laboratory animal welfare People's Republic of China National Standard GB/T 35892–2018.[22] Female 5–7 weeks old BALB/c mice (Shanghai Laboratory Animal Center, CAS) were maintained in individually ventilated caging systems at 19°C to 23°C, with a 12-h light-dark cycle. At autopsy, heart, lung, spleen, brain, uterus and ovary were removed, fixed in formalin, and embedded in paraffin.

Clinical Specimens

Chorionic tissues were collected from 8 aborted pregnant women at the Obstetrics and Gynecology Hospital. The placenta is a temporary maternal-fetal organ that provides the nutrients and oxygen to the baby for development and growth. The placenta is usually expelled within 15–30 min after the child is born, thus we obtained 8 placentas from women giving birth. Ethical approval from the Obstetrics and Gynecology Hospital Research Ethics Committee and all enrolled volunteers' written informed consent were obtained.

Human cardiac samples used in this study were obtained from Zhongshan Hospital, Fudan University, with the approval of the Research Ethics Committee from this hospital. The donated heart was obtained from a trauma victim with no apparent adverse heart condition, and written informed consent was obtained from the next of kin.

Immunofluorescence Staining

Immunostaining was carried out using recommended protocol and imaging was performed on a Leica TCS-SP5 confocal microscope. Briefly, cells were fixed with 4% paraformaldehyde min and then blocked in 5% goat serum (Biotech Well), followed by primary antibody incubation overnight at 4°C. The primary antibody was

monoclonal mouse anti-HCGR (1:500, Abcam). Following primary antibody incubation and washes, cells were incubated with Cy3-conjugated goat anti-mouse IgG (Jackson ImmunoResearch) for 30 min in the dark at room temperature. DAPI (Sigma-Aldrich) was used for nuclear identification. Cells were observed using a Leica TCS-SP5 confocal microscope after staining.

Western Blotting

Total protein was extracted by lysing cells in RIPA buffer containing protease inhibitor. Protein samples were separated on 10% sodium dodecyl sulfate polyacrylamide gel electrophoresis (SDS-PAGE) and transferred to polyvinylidene fluoride (PVDF) membranes. After blocking with 5% non-fat milk in TBS-T for 1 h, membranes were incubated with the primary antibody. The following antibodies were used: anti-HCGR (1:1000, Abcam), β-actin (1:5000, Genescript) and anti-GAPDH (1:1000, CST) were used as loading controls. Goat-anti-mouse and goat-anti-rabbit IgG conjugated to horseradish peroxidase (HRP) (1:5000, Cwbiotech) were used as the secondary antibodies. Proteins were detected using ECL detection system (Pierce).

Immunohistochemistry Staining

Formalin-fixed, paraffin-embedded tissues were cut into 4-μm sections. Following deparaffinization, sections were rehydrated and subjected to antigen retrieval by microwaving in 10 mM sodium citrate (pH 6) for 10 min. Sections were incubated at 4°C overnight with antibodies against HCGR (1:500, Abcam). Immunostaining was performed using EnVision™ Detection Kit, Peroxidase/DAB, Rabbit/Mouse (DakoCytomation) according to the manufacturer's instructions. Protein staining was evaluated under a light microscope at 200× magnification (Leica).

Preparation of HCG81-NP and FITC-Labeled HCG81-NP

Peptide HCGβ 81–95 (SYAVALSCQCALCRR) and peptide FITC-labeled HCGβ 81–95 (FITC-SYAVALSCQCALCRR) were synthesized and purified by high-performance liquid chromatography (HPLC). Nanoparticles were prepared with maleimide-PEG-PLA, which were synthesized by a ring-opening polymerization of lactide initiated by the hydroxyl group of methoxy poly (ethylene glycol), using the emulsion/solvent evaporation technique.[23,24]

MTX-NP was prepared by an oil-water emulsification solvent evaporation method. MTX (10 mg) was dissolved in 2 mL of dichloromethane containing 2.5% maleimide-PEG-PLA and MPEG-PLA. Add organic phase into 20 mL of 1% sodium cholate aqueous solution and sonicated. Then, stir the emulsion for 1 h at 40°C to obtain MTX-NPs (5 mg/mL).

To prepare HCG81-NP, the mixture of HCGβ 81–95 peptide and nanoparticles (the molar ratio of HCGβ 81–95 peptide and maleimide was 1:1) was magnetically stirred overnight. The reaction mixture was then isolated on a Sepharose CL-4B column (GE Healthcare) by elution with HEPES buffer. The milky HCG81-NP fractions were collected by centrifugation. The working model of HCG81-NP was shown in Supplementary Figure S4.

Nanoparticle Characterization

The morphology of nanoparticles was evaluated by transmission electron microscope (TEM) (Hitachi). NPs were diluted in distilled water to make a 1 mg/mL suspension. The TEM sample was prepared by placing a drop of the nanoparticle suspension onto a copper grid coated with carbon. After having been dried, the sample was observed and photographed directly. Nuclear magnetic resonance spectroscopy (NMR) spectra were carried out using AvanceIII 500 MHz NMR spectrometer (Bruker). The absolute molecular weight of the NPs was measured by a gel permeation chromatography (GPC, Waters). The samples were dissolved in 0.5 M sodium acetate buffer (pH 6.0), and the flow rate was 0.5 mL/min. The injection volume was 0.2 mL (5 mg/mL).

To determine the content of MTX, MTX-NP was dissolved in methanol and analyzed via HPLC system. The release of MTX from NPs was measured by adding 1 mL NP-PTX into a dialysis cassette (Thermo Scientific) and dialyzing in 300 mL of PBS (pH 7.4). The dialysis system was stirred at 75 rpm for 2 h at room temperature, then change the dialysis buffer and dialyze for another 2 h. The amount of MTX released in each time interval was analyzed using HPLC method.

Peptide Binding Assay

To examine whether HCGβ 81–95 peptide conjugated specifically to HCGR-expressed cell lines, JEG-3 and JAR cells were incubated in PBS with 10 μM FITC-labeled HCGβ 81–95 peptide for 30 min. Cells were then rinsed with PBS buffer and fixed with 4% paraformaldehyde.

After mounting, cells were examined by fluorescence microscope (Leica).

Proliferation Assay

Cell proliferation was determined over a 72 h period by the Cell Counting Kit-8 (Dojindo). After a 24 h serum withdrawal, 2×10^4 cells were plated into 96-well plates in 0.1 mL growth medium with MTX, NP-MTX, or HCG81-NP-PTX of different concentrations (0 nM, 200 nM, 400 nM and 800 nM). The CCK-8 solution was added 10 μL/well, cells were subsequently incubated for 2 h at 37°C. Then, the plates were read on a multiwell scanning spectrophotometer (Multiskan MK3, Thermo Fisher Scientific) at 450 nm, with wavelength correction at 630 nm.

Cell Cycle Analysis

To determine cell cycle profile, 2×10^6 cells were harvest and fixed in cold 70% ethanol at −20°C overnight. Then, wash cells in PBS and discard the supernatant. Cells were treated with 100 μL of 100 μg/mL RNase ribonuclease I at 37°C for 30 min. Samples were incubated with 500 μL of 50 μg/mL PI (light sensitive) at room temperature for 10 min, then samples were transferred to Falcon tubes and analyzed by FACScan. The percentages of cells occupying in the G0/G1, S, and G2/M phases were calculated from the resulting DNA histogram with CellQuest software (BD Biosciences).

Statistical Analysis

All in vitro experiments were conducted in triplicate and carried out on three separate occasions. Numerical data were expressed as means ± standard deviation. Statistically significant differences between the means for the different groups were determined by two-tailed unpaired Student's *t*-test, and results with *P* values of less than 0.05 were considered significant.

Results

Expression Levels of HCGR Protein

To evaluate the possibility of using HCGR as a therapeutic target, we first examined HCGR expression on human genital system cancer cell lines via immunofluorescence assay. HCGR expression was not detected in ovarian cancer cell line Caov-3, whereas choriocarcinoma cell lines JAR and JEG-3 exhibited positive staining for HCGR (Figure 1A). This high expression rate indicated that HCGR could be used as the therapeutic target in our system.

Next, we evaluated HCGR expression in a panel of human cell lines using Western blot experiment, including normal cells HOK and HCASMC, immortalized noncancerous cell line HEK-293 and HTR8/sev8, as well as cancerous cell lines THP-1, JEG-3, JAR and Caov-3. HCGR protein level was undetectable in HOK, HCASMC, THP-1 and HEK-293 cells, slightly expressed in human trophoblast cell line HTR8/sev8 and ovarian cancer cell line Caov-3, whereas strongly expressed in human choriocarcinoma cell lines JAR and JEG-3 (Figure 1B). Immunohistochemistry staining showed that HCGR protein was not expressed in the heart, lung, spleen, and brain of BALB/c mice while slightly expressed in reproductive organs (uterus and ovary) (Figure 1C). Western blot assay confirmed the expression levels of HCGR in different tissues of BALB/c mice (Figure 1D).

We further investigated HCGR expression level in clinical specimens obtained from a cohort 8 aborted pregnant women and 8 women giving birth. A high expression level of HCGR protein had been detected both in chorion and placenta tissues. Human cardiac tissue obtained from a trauma victim was used as negative control here, and HCGR expression was rarely expressed in heart sample (Figure 1E). Therefore, an HCGR-targeted therapeutic strategy could be utilized to deliver drugs specifically to localized tumor sites.

Characterization of Nanoparticles and Covalent Coupling of the HCGβ Peptide to the Nanoparticles

HCGβ81-95 and FITC-labeled HCGβ81-95 were synthesized and checked for molecular weights by HPLC as well as mass spectrometry (Supplementary Figure S1). We also examined the shape and size of these nanoparticles using transmission electron microscopy (TEM). The nanoparticles (NP) and HCGβ 81-NP loaded with or without MTX were spherical and had a regular size from 80 to 120 nm. Figure 2A showed that the average particle size of HCGβ 81-NP loaded with MTX was 112.6 nm, and polydispersity index (PDI) was 0.143. Their molecular weight and NP distribution were identified by gel permeation chromatography (GPC) (Figure 2B). The retention time of HCGβ 81-NP loaded with MTX was 22.5 min. Nuclear magnetic resonance spectroscopy (NMR) data were exhibited in Figure 2C. The lower panel showed the magnetic

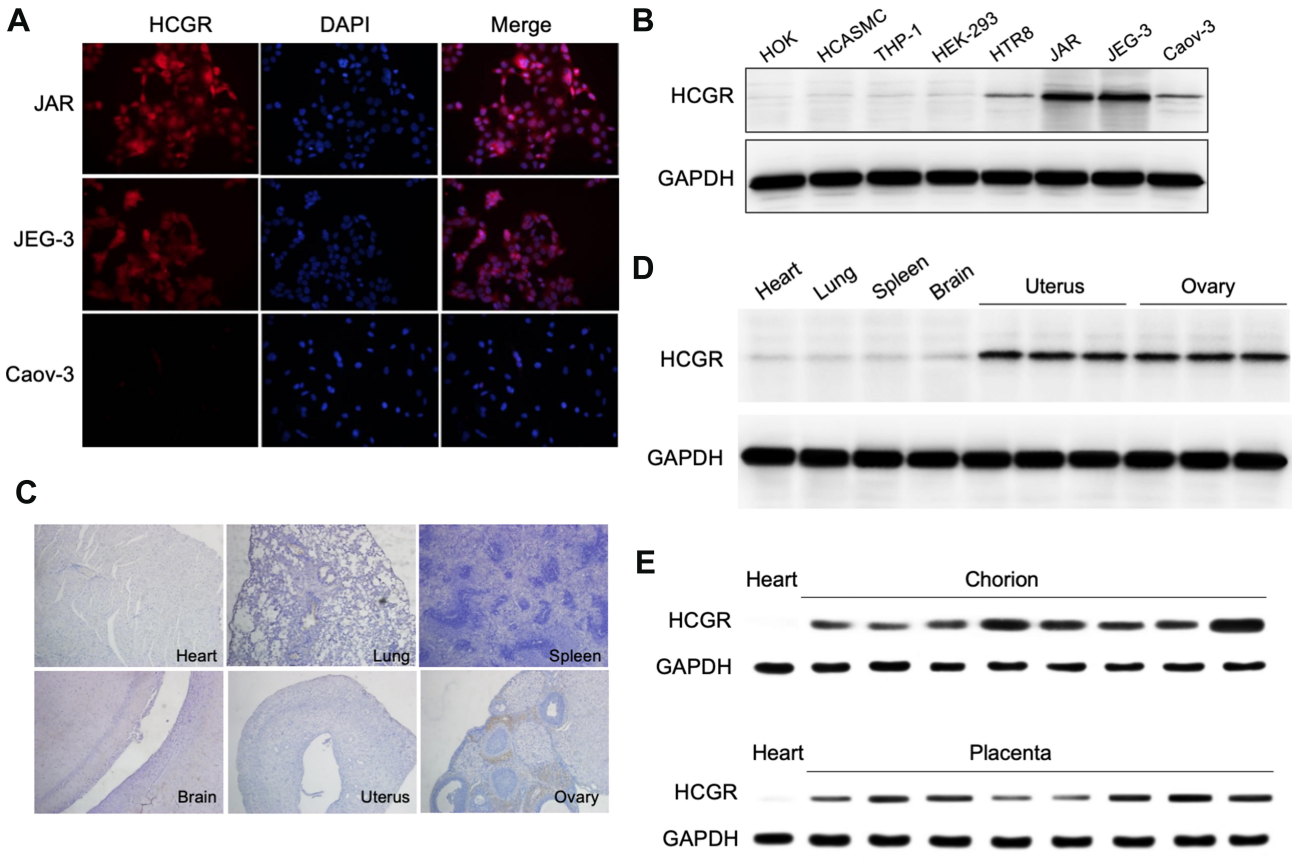

Figure 1 Expression levels of HCGR protein. (**A**) Cancer cells were stained with anti-HCGR (red) antibody, and cell nuclei were stained with DAPI (blue). Confocal images were collected to analyze the HCGR protein expression on human genital system cancer cell lines. (**B**) HCGR expression in a panel of human cell lines were examined using Western blot experiment. (**C**) HCGR expression were detected in the heart, lung, spleen, brain, uterus and ovary of BALB/c mice via immunohistochemistry staining. (**D**) Western blot assay presented the expression levels of HCGR in different tissues of BALB/c mice. (**E**) HCGR expression level were evaluated in a cohort of human clinical specimens.

resonance image of a PEG-PLA nanoparticle without HCG peptide modification, while the upper panel presented d peak disappeared, indicating that the HCGβ 81–95 polypeptide was connected to the PEG-PLA nanoparticles and the nanoparticles were loaded with MTX. Taken together, the size distribution coefficient of nanoparticles modified by HCGβ peptide loaded with or without MTX met the experimental requirements.

Peptide HCGβ81-95 Specifically Bonded to Human Choriocarcinoma Cells and HCG81-NP Efficiently Delivered MTX to Choriocarcinoma Cells

To figure out whether HCGβ 81–95 peptide could conjugate specifically to choriocarcinoma cell lines which are highly expressing HCGR, FITC-labeled HCGβ 81–95 peptide was incubated with either JEG-3 or JAR cells. Fluorescence microscopy exhibited that this peptide could bind to the HCGR-positive JEG-3 and JAR cells (Figure 3A and B). Next, we conjugated MTX to HCG81-NP and examined its antitumor effect in vitro. In Supplementary Figure S2, encapsulation efficiency was measured using a UV spectrophotometer. Formulations prepared from PEG-PLA coated NPs showed high MTX loading (~10.2%) and encapsulation efficiency (~68%).

HCG81-NP-MTX Inhibited Cell Proliferation and Reduced G0/G1 to S Phase Transition in Choriocarcinoma Cells

Chemotherapy drug MTX inhibits dihydrofolate reductase, which is essential for cell growth and proliferation. Here we tested whether HCG81-NP could deliver MTX to HCG receptor-positive choriocarcinoma cells to specifically and efficiently suppress cell proliferation. The proliferation rate of JEG-3 and JAR cells remained unchanged by

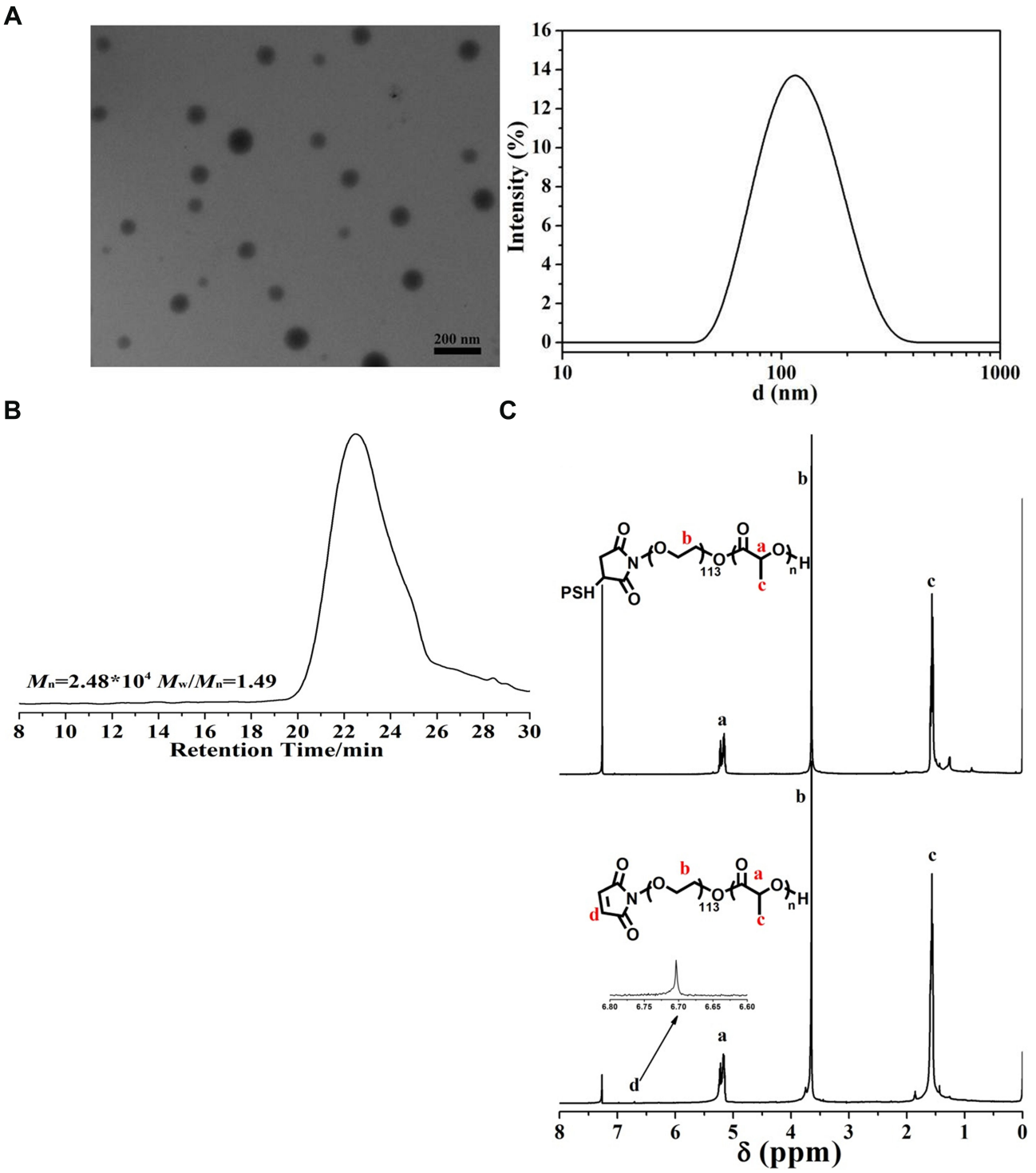

Figure 2 Characterization of nanoparticles and covalent coupling of HCGβ peptide to the nanoparticles. (**A**) HCGβ 81-nanoparticles pictures in transmission electron microscopy and size distribution. (**B**) Gel permeation chromatography was used to detect the molecular weight and distribution of nanoparticles. (**C**) HCGβ 81-NP with or without MTX loaded were measured by nuclear magnetic resonance spectroscopy.

different concentrations of HCG81-NP treatment ($P > 0.05$), indicating that nanoparticles modified by HCGβ peptide maintained the phenotype of choriocarcinoma cells in vitro (Supplementary Figure S3). Different concentrations of MTX, NP-MTX, or HCG81-NP-MTX were then added to human choriocarcinoma cells and incubated for 72 h, respectively. Cell proliferation assays showed there was approximately a 75% reduction of cell

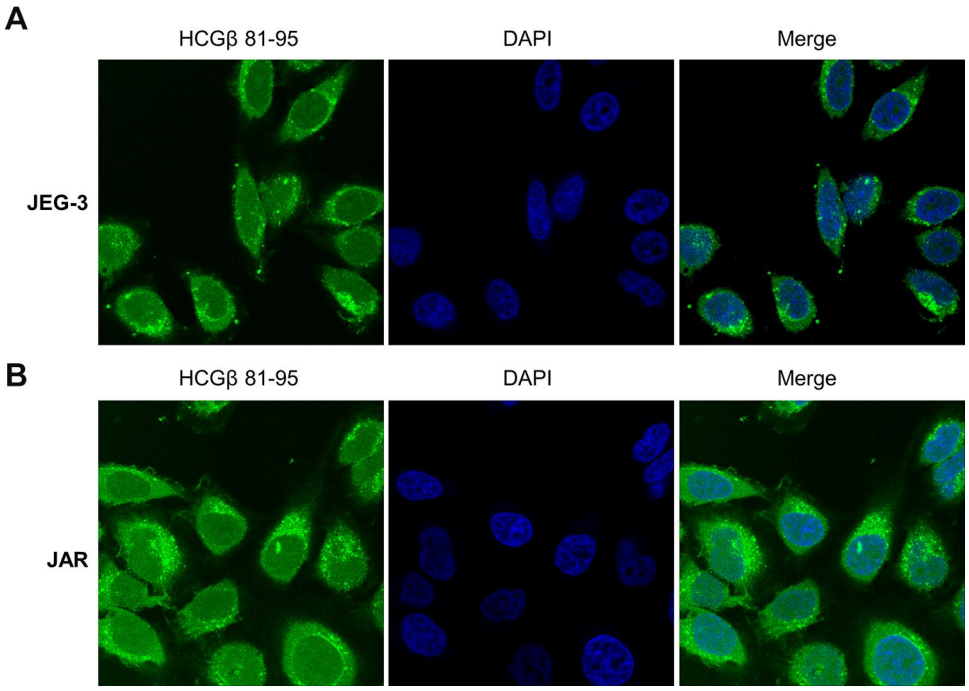

Figure 3 Peptide HCGβ81-95 specifically bonded to human choriocarcinoma cells. Fluorescence microscopy exhibited HCGβ 81–95 peptide conjugated specifically to JEG-3 cells (**A**) and JAR cells (**B**).

proliferation rate in JEG-3 cells and a 60% reduction in JAR cells, respectively, in response to 800 nM HCG81-NP-MTX ($P<0.05$, *t*-test; Figure 4A and B). Next, we performed a cell cycle analysis to determine whether HCG81-NP-MTX treatment inhibited cell growth via alteration of the cell cycle. Cell cycles of JEG-3 and JAR cells were monitored by fluorescence-activated cell sorting (FACS) (Figure 5A and B). As expected, HCG81-NP-MTX treatment altered the cell cycle by arresting the G_0/G_1 to S phase transition (Figure 5C and D). Taken together, our data suggested that although nanoparticles coupled with MTX could already facilitate MTX uptake by cells, HCGβ 81–95 peptide–coupled NP-MTX could target HCGR expressing cells more specifically and efficiently in vitro.

Discussion

Choriocarcinoma is one of the highest degrees of malignant trophoblastic tumors, and chemotherapy is so far the most effective therapy. HCG is a glycoprotein hormone that is produced by syncytiotrophoblasts of human placentas as well as gestational trophoblastic diseases which

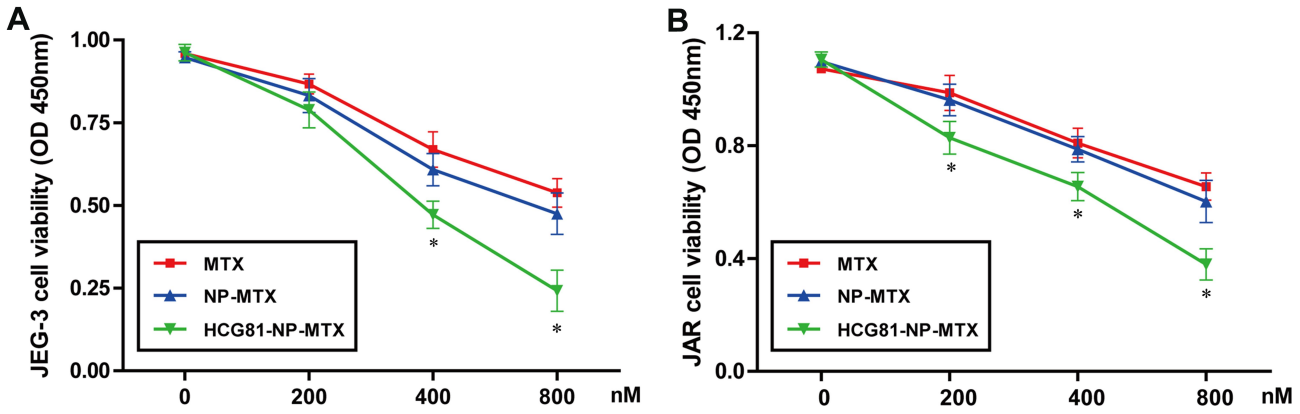

Figure 4 HCG81-NP-MTX inhibited cell proliferation of JEG-3 and JAR cells in a dosage-dependent manner. The growth of MTX, NP-MTX or HCG81-NP-MTX treated JEG-3 cells (**A**) and JAR cells (**B**) were analyzed using the CCK-8 kit. * denotes significant difference from nontreatment controls ($P<0.05$) for mean±SD of five samples per condition. Error bars represent ± SD.

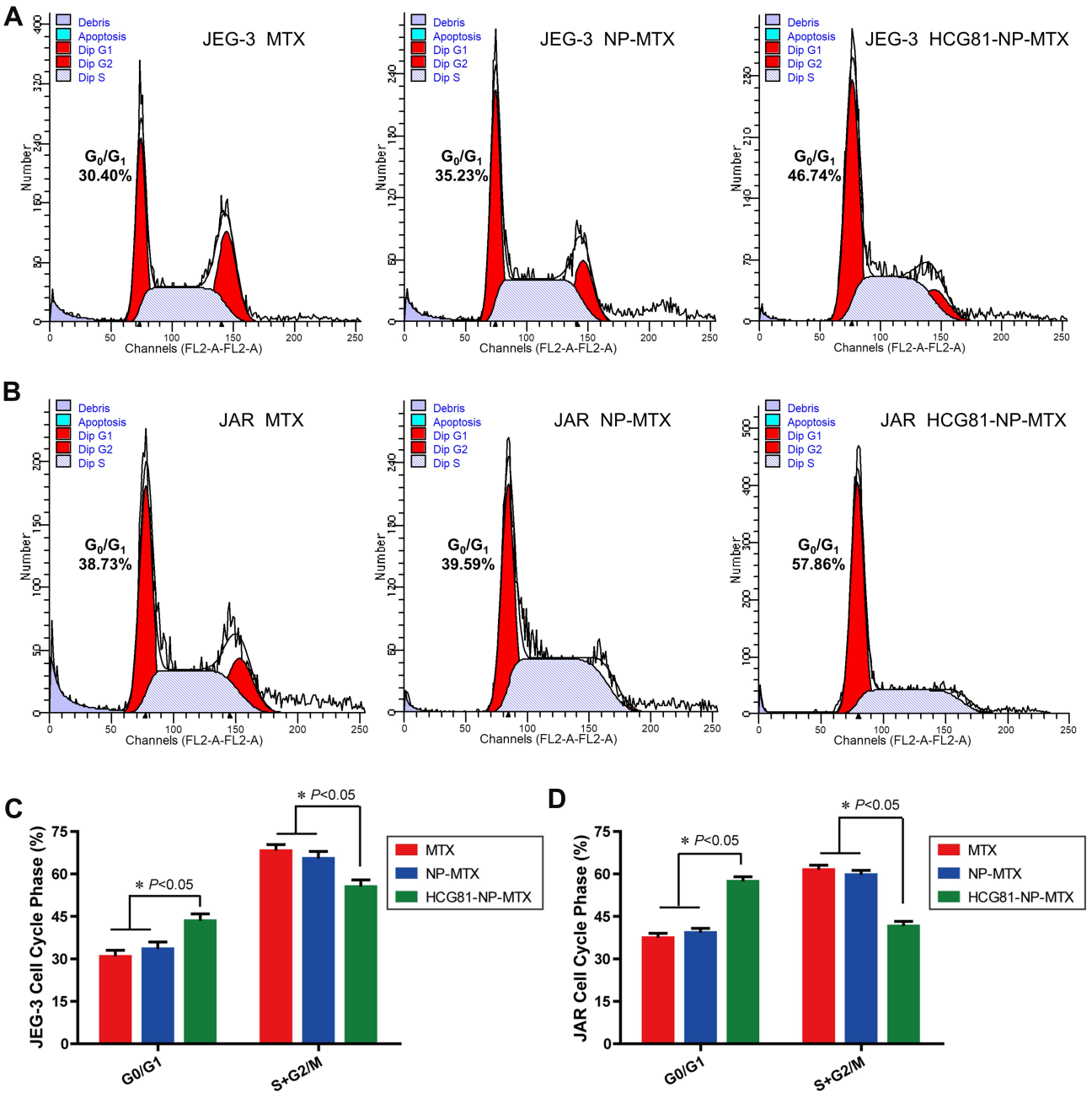

Figure 5 HCG81-NP-MTX treatment reduced G0/G1 to S phase transition in choriocarcinoma cells. Cell cycle profiles of JEG-3 (**A**) and JAR (**B**) was analyzed by FACScan. (**C**, **D**) The summary graphs were presented for the cell cycle assay. Data represent the mean±SD of three independent experiments (*$P< 0.05$).

including GTN.[25] HCG is a heterodimer composed of the α-hCG and β-hCG subunits. The α (alpha) subunit is 92 amino acids long while the β (beta) subunit contains 145 amino acids, encoded by six highly homologous genes that are arranged in tandem and inverted pairs on chromosome 19q13.3.[26] The receptor of HCG is a seven transmembrane G protein-coupled receptor, named HCGR. Morbeck et al identified hCG beta 81–95 was extraordinarily critical for maximal binding of the hormone to its receptor.[21] In this study, we developed a novel active targeted therapeutic system, HCG81-NP, and showed its potential as a promising drug delivery strategy.

Compared with commonly used monoclonal antibody agents, peptides are smaller, cheaper, easier to prepare, and have lower immunogenicity. Peptide HCGβ 81–95 was chosen as a target-specific ligand due to its high affinity to HCGR. This peptide was covalently attached to PEG-PLA nanoparticles. Particulate carriers with diameters of

approximately 100 nm have been widely used to improve the distribution and tumor accumulation of cancer drugs.[27,28] MTX is a folate analog with anti-inflammatory effects due to the blockage of the synthesis of purine and pyrimidine precursors of DNA and RNA, leading to inhibition of cell proliferation and induction of cell death. Moreover, MTX is almost insoluble in water, ethanol, chloroform, and ethyl ether, and is a hydrophobic drug suitable for inclusion in amphoteric molecular nanoparticles.[5] However, common MTX side effects may include diarrhea, vomiting, bloody urine, fever, leukocytopenia, unusual bleeding, and so on.[8,28] Thus, we encapsulated MTX in PEG-PLA diblock copolymer nanoparticles for targeted chemotherapy.

Although nanoparticles coupled with MTX could already facilitate MTX uptake by cells, HCG81-NP-MTX was much more effective at lower concentrations in this study. We conjugated MTX to HCGβ 81–95 peptide provided as a specific target for cytotoxic drug delivery to HCG receptor-positive choriocarcinoma cells. HCG81-NP-MTX exhibited marked suppression of cell proliferation rate in JEG-3 and JAR cells, compared with NP-MTX as well as NP. Cell cycle analysis showed that HCG81-NP-MTX treatment induced cell cycle arrest at the G_0/G_1 to S phase transition. In summary, this study suggests one active targeting therapy system of choriocarcinoma, which hugely improved chemotherapy efficacy and provided a theoretical basis for the treatment of malignant trophoblastic tumors.

Conclusion

In this study, we designed an active targeting therapy system of choriocarcinoma, significantly improved chemotherapy efficacy, dramatically reduced the toxic reaction, and provided a theoretical basis for the treatment of malignant trophoblastic tumors.

Abbreviations

GTN, gestational trophoblastic neoplasia; HCG, human chorionic gonadotropin; HCGR, human chorionic gonadotropin receptor; LHCGR, luteinizing hormone/choriogonadotropin receptor; GPCR, G protein coupled receptor; MTX, methotrexate; HCG81-NP, HCGβ81-95 polypeptide conjugated nanoparticles; PEG, poly(ethylene glycol); PLA, poly (lactic acid); HPLC, high-performance liquid chromatography; PDI, polydispersity index; TEM, transmission electron microscope; NMR, nuclear magnetic resonance spectroscopy; GPC, gel permeation chromatography; SDS-PAGE, sodium dodecyl sulfate polyacrylamide gel electrophoresis; PVDF, polyvinylidene fluoride; HRP, horseradish peroxidase; FACS, fluorescence-activated cell sorting.

Acknowledgment

We sincerely thank Prof. Juying Qian for offering precious human cardiac tissue and Shuhui Sun for her technical skill in flow cytometry. Many technical assistance and helpful discussions with Lei Xiong are also gratefully acknowledged.

Funding

This work was supported by Health Commission Project of Shanghai Municipality (201344095) and Clinical Research Project of Shanghai Municipal Health Commission (20204Y0115).

Disclosure

The authors declare no conflicts of interest.

References

1. Lurain JR, Elfstrand EP. Single-agent methotrexate chemotherapy for the treatment of nonmetastatic gestational trophoblastic tumors. *Am J Obstet Gynecol*. 1995;172(2):574–579. doi:10.1016/0002-9378(95)90575-8
2. Lurain JR. Gestational trophoblastic disease II: classification and management of gestational trophoblastic neoplasia. *Am J Obstet Gynecol*. 2011;204(1):11–18.
3. Braga A, Mora P, de Melo AC, et al. Challenges in the diagnosis and treatment of gestational trophoblastic neoplasia worldwide. *World J Clin Oncol*. 2019;10(2):28–37.
4. Bleyer WA. Methotrexate: clinical pharmacology, current status and therapeutic guidelines. *Cancer Treat Rev*. 1977;4(2):87–101.
5. Frei E, Jaffe N, Tattersall MH, Pitman S, Parker L. New approaches to cancer chemotherapy with methotrexate. *N Engl J Med*. 1975;292(16):846–851.
6. Green MR, Chowdhary S, Lombardi KM, Chalmers LM, Chamberlain M. Clinical utility and pharmacology of high-dose methotrexate in the treatment of primary CNS lymphoma. *Exp Rev Neurother*. 2006;6(5):635–652.
7. Jolivet J, Cowan KH, Curt GA, Clendeninn NJ, Chabner BA. The pharmacology and clinical use of methotrexate. *N Engl J Med*. 1983;309(18):1094–1104.
8. Widemann BC, Adamson PC. Understanding and managing methotrexate nephrotoxicity. *Oncologist*. 2006;11(6):694–703.
9. Ramos AP, Cruz MAE, Tovani CB, Ciancaglini P. Biomedical applications of nanotechnology. *Biophys Rev*. 2017;9(2):79–89.
10. Prasad M, Lambe UP, Brar B, et al. Nanotherapeutics: an insight into healthcare and multi-dimensional applications in medical sector of the modern world. *Biomed Pharmacother*. 2018;97:1521–1537. doi:10.1016/j.biopha.2017.11.026
11. Patra JK, Das G, Fraceto LF, et al. Nano based drug delivery systems: recent developments and future prospects. *J Nanobiotechnol*. 2018;16(1):71.
12. Senapati S, Mahanta AK, Kumar S, Maiti P. Controlled drug delivery vehicles for cancer treatment and their performance. *Signal Transduct Target Ther*. 2018;3:7.
13. Zhang XY, Chen J, Zheng YF, et al. Follicle-stimulating hormone peptide can facilitate paclitaxel nanoparticles to target ovarian carcinoma in vivo. *Cancer Res*. 2009;69(16):6506–6514.

14. Bazile D, Prud'homme C, Bassoullet MT, Marlard M, Spenlehauer G, Veillard M. Stealth Me.PEG-PLA nanoparticles avoid uptake by the mononuclear phagocytes system. *J Pharm Sci*. 1995;84(4):493–498.
15. Meunier M, Goupil A, Lienard P. Predicting drug loading in PLA-PEG nanoparticles. *Int J Pharm*. 2017;526(1–2):157–166.
16. Hong S, Zhang X, Chen J, Zhou J, Zheng Y, Xu C. Targeted gene silencing using a follicle-stimulating hormone peptide-conjugated nanoparticle system improves its specificity and efficacy in ovarian clear cell carcinoma in vitro. *J Ovarian Res*. 2013;6(1):80.
17. Lei ZM, Rao CV, Ackerman DM, Day TG. The expression of human chorionic gonadotropin/human luteinizing hormone receptors in human gestational trophoblastic neoplasms. *J Clin Endocrinol Metab*. 1992;74(6):1236–1241.
18. Choi J, Smitz J. Luteinizing hormone and human chorionic gonadotropin: origins of difference. *Mol Cell Endocrinol*. 2014;383 (1–2):203–213.
19. Lei ZM, Reshef E, Rao V. The expression of human chorionic gonadotropin/luteinizing hormone receptors in human endometrial and myometrial blood vessels. *J Clin Endocrinol Metab*. 1992;75 (2):651–659.
20. Casarini L, Riccetti L, De Pascali F, et al. Estrogen modulates specific life and death signals induced by LH and hCG in human primary granulosa cells in vitro. *Int J Mol Sci*. 2017;18:5.
21. Morbeck DE, Roche PC, Keutmann HT, McCormick DJ. A receptor binding site identified in the region 81-95 of the beta-subunit of human luteinizing hormone (LH) and chorionic gonadotropin (hCG). *Mol Cell Endocrinol*. 1993;97(1–2):173–181.
22. MacArthur Clark JA, Sun D. Guidelines for the ethical review of laboratory animal welfare People's Republic of China National Standard GB/T 35892-2018 [Issued 6 February 2018 Effective from 1 September 2018]. *Animal Model Exp Med*. 2020;3:103–113.
23. Tobio M, Gref R, Sanchez A, Langer R, Alonso MJ. Stealth PLA-PEG nanoparticles as protein carriers for nasal administration. *Pharm Res*. 1998;15(2):270–275.
24. Ruan G, Feng SS. Preparation and characterization of poly(lactic acid)-poly(ethylene glycol)-poly(lactic acid) (PLA-PEG-PLA) microspheres for controlled release of paclitaxel. *Biomaterials*. 2003;24 (27):5037–5044.
25. Braunstein GD, Vaitukaitis JL, Carbone PP, Ross GT. Ectopic production of human chorionic gonadotrophin by neoplasms. *Ann Intern Med*. 1973;78(1):39–45.
26. Talmadge K, Vamvakopoulos NC, Fiddes JC. Evolution of the genes for the beta subunits of human chorionic gonadotropin and luteinizing hormone. *Nature*. 1984;307(5946):37–40.
27. Cabral H, Matsumoto Y, Mizuno K, et al. Accumulation of sub-100 nm polymeric micelles in poorly permeable tumours depends on size. *Nat Nanotechnol*. 2011;6(12):815–823.
28. Caster JM, Yu SK, Patel AN, et al. Effect of particle size on the biodistribution, toxicity, and efficacy of drug-loaded polymeric nanoparticles in chemoradiotherapy. *Nanomedicine*. 2017;13(5):1673–1683.